




## Article

# Sustained Release of Co-Amorphous Matrine-Type Alkaloids and Resveratrol with Anti-COVID-19 Potential

Dandan Hu <sup>1</sup>, Xin Chen <sup>1</sup>, Duanxiu Li <sup>2,3</sup>, Hailu Zhang <sup>2</sup>, Yanwen Duan <sup>1,4,5</sup> and Yong Huang <sup>1,5,\*</sup>

<sup>1</sup> Xiangya International Academy of Translational Medicine, Central South University, Changsha 410013, China; dandanhu@yeah.net (D.H.); xchen2016@sinano.ac.cn (X.C.); ywduan66@csu.edu.cn (Y.D.)

<sup>2</sup> Laboratory of Magnetic Resonance Spectroscopy and Imaging, Suzhou Institute of Nano-Tech and Nano-Bionics, Chinese Academy of Sciences, Suzhou 215123, China; dxli2016@sinano.ac.cn (D.L.); hlzhang2008@sinano.ac.cn (H.Z.)

<sup>3</sup> Guangdong Institute of Semiconductor Micro-Nano Manufacturing Technology, Foshan 528200, China

<sup>4</sup> Hunan Engineering Research Center of Combinatorial Biosynthesis and Natural Product Drug Discovery, Changsha 410011, China

<sup>5</sup> National Engineering Research Center of Combinatorial Biosynthesis for Drug Discovery, Changsha 410011, China

\* Correspondence: jonghuang@csu.edu.cn; Tel.: +86-731-82650539

**Abstract:** Matrine (MAR), oxymatrine (OMAR), and sophoridine (SPD) are natural alkaloids with varying biological activities; matrine was recently used for the treatment of coronavirus disease 2019 (COVID-19). However, the short half-lives and rapid elimination of these matrine-type alkaloids would lead to low oral bioavailability and serious side effects. Herein, resveratrol (RES) was selected as a co-former to prepare their co-amorphous systems to improve the therapeutic index. The formation of co-amorphous MAR-RES, OMAR-RES, and SPD-RES was established through powder X-ray diffraction and modulated temperature differential scanning calorimetry. Furthermore, Fourier transform infrared spectroscopy and NMR studies revealed the strong molecular interactions between resveratrol and these alkaloids, especially OMAR-RES. Matrine, oxymatrine, and sophoridine in the co-amorphous systems showed sustained release behaviors in the dissolution experiments, due to the recrystallization of resveratrol on the surface of co-amorphous drugs. The three co-amorphous systems exhibited excellent physicochemical stability under high relative humidity conditions. Our study not only showed that minor structural changes of active pharmaceutical ingredients may have distinct molecular interactions with the co-former, but also discovered a new type of sustained release mechanism for co-amorphous drugs. This promising co-amorphous drug approach may present a unique opportunity for repurposing these very promising drugs against COVID-19.

**Keywords:** co-amorphous systems; sustained-release; COVID-19; matrine-type alkaloids; resveratrol



**Citation:** Hu, D.; Chen, X.; Li, D.; Zhang, H.; Duan, Y.; Huang, Y. Sustained Release of Co-Amorphous Matrine-Type Alkaloids and Resveratrol with Anti-COVID-19 Potential. *Pharmaceutics* **2022**, *14*, 603. <https://doi.org/10.3390/pharmaceutics14030603>

Academic Editor: Peter Timmins

Received: 15 January 2022

Accepted: 7 March 2022

Published: 10 March 2022

**Publisher's Note:** MDPI stays neutral with regard to jurisdictional claims in published maps and institutional affiliations.

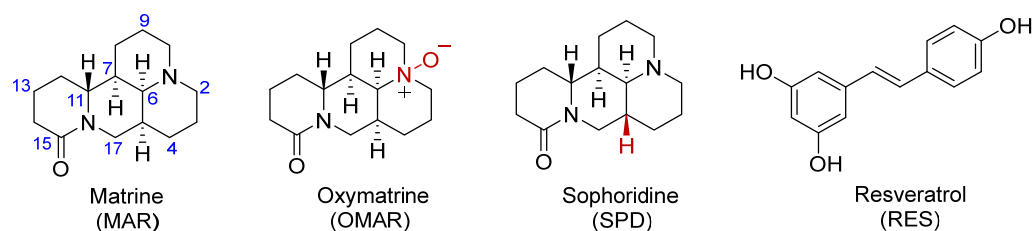


**Copyright:** © 2022 by the authors. Licensee MDPI, Basel, Switzerland. This article is an open access article distributed under the terms and conditions of the Creative Commons Attribution (CC BY) license (<https://creativecommons.org/licenses/by/4.0/>).

## 1. Introduction

The coronavirus disease 2019 (COVID-19) pandemic caused by severe acute respiratory syndrome coronavirus 2 (SARS-CoV-2) has led to over 5 million deaths worldwide as of early December 2021 [1]. The rapidly developed various types of vaccines against SARS-CoV-2, such as the inactivated virus COVID-19 vaccine CoronaVac and the Pfizer-BioNTech and Moderna COVID-19 mRNA vaccines, have shown effectiveness against SARS-CoV-2 spread and significantly reduced the severity and death rate among more vulnerable populations [2]. However, the rapid evolving variants of SARS-CoV-2 may render these vaccines less effective. Drug reposition is a rapid approach to develop life-saving medications against COVID-19 in a global health crisis. For example, high throughput screenings of various drug collections have yielded multiple drug leads against viral replication of SARS-CoV-2, including PIKfyve kinase inhibitor apilimod, multiple cysteine protease inhibitors, as well as farnesyltransferase inhibitor tipifarnib and phosphatidylinositol 3-kinase inhibitor omipalisib [3,4].

Natural products have great potential to treat SARS-CoV-2 [5], among which plant-derived medicines, including the lung cleansing and detoxifying decoction with 21 ingredients, have been used against COVID-19 in China [6,7]. Matrine (MAR), a representative quinolizidine alkaloid from *Sophora flavescens* Ait, has been used to treat chronic hepatitis and enteritis for years in China (Scheme 1, Table S1) [8]. Impressively, matrine was used to treat 40 COVID-19 patients, in addition to other recommended treatment regimens, such as antiviral drugs abidol or lopinavir and ritonavir in early 2020 [9]. These treatments markedly reduced the fibrotic and grid-like lesions in the lungs of patients by chest computed tomography scan and cleared SARS-CoV-2 from patients within 10 days of the combination therapy. Furthermore, the mortality rate among hospitalized COVID-19 patients strongly correlated with the autoimmunity level to annexin A2 [10], suggesting its importance in SARS-CoV-2 pathogenicity [11]. Matrine was shown to directly target annexin A2 by a photo-affinity labeling approach [12], while very recent network pharmacological studies suggested that matrine may also have varying targets in cellular signaling pathways [13–15]. Oxymatrine (OMAR) and sophoridine (SPD, Scheme 1) are matrine-type alkaloids isolated from *S. flavescens* Ait with promising biological activities [16,17], including antiviral activity [18,19]. Resveratrol (RES) is a plant polyphenol, which has also been used to treat COVID-19 patients with mild symptoms or as adjuvant supplements due to its anti-SARS-CoV-2 and anti-inflammatory activities [20,21].



**Scheme 1.** Molecular structures of MAR, OMAR, SPD, and RES.

However, matrine was given to COVID-19 patients via intravenous infusion [9], suggesting its poor pharmacokinetic properties, which may result in poor patient compliance and persistence, as well as unsatisfactory outcomes. Several studies of oral administration of matrine, oxymatrine, and sophoridine in model animals showed that their absolute bioavailability was 17.1% [22], 6.79% [23], and 2.32% [24], with half-lives of  $1.53 \pm 0.53$  [22],  $6.45 \pm 1.07$  [23], and  $4.67 \pm 1.50$  h [24], respectively. Drug co-amorphization is an emerging technology to improve the physicochemical properties of oral drugs [25], which is a single-phase amorphous system formed between an active pharmaceutical ingredient and one or more low molecular weight compounds named co-formers [26]. For example, it may improve the bioavailability of poorly water-soluble drugs by increasing their solubilities, such as indomethacin and apigenin [27,28]. However, co-amorphization of drugs would not always enhance their solubilities or dissolution rates. The solubility of certain drugs in co-amorphous systems may be impacted by many factors, including co-amorphization, the solubilities of co-formers, and intermolecular interactions between drugs and co-formers. Hence, the solubilities and dissolution rates of drugs in co-amorphous systems may be decreased, which provides an excellent opportunity for the sustained release of drugs. We and others have recently discovered that certain co-amorphous drug delivery systems exhibited sustained release behaviors, including lurasidone hydrochloride, indomethacin/paracetamol [29,30], sinomenine/phenolic acids, and sinomenine/nonsteroidal anti-inflammatory drugs indomethacin, naproxen, and sulindac [31,32]. Therefore, we envision that a new sustained release-based strategy for matrine-type alkaloids is needed to realize their full translational potential in COVID-19 therapy.

In this study, we test the hypothesis if resveratrol can be used as a new co-former for the formation of co-amorphous drug systems with matrine, oxymatrine, and sophoridine, due to the potential synergistic effects against SARS-CoV-2. These new solid formulations have been prepared and systematically characterized by powder X-ray diffraction (PXRD),

Fourier transform infrared spectroscopy (FTIR), modulated temperature differential scanning calorimetry (mDSC), scanning electron microscopy (SEM), and nuclear magnetic resonance (NMR) spectroscopy. Further, they showed distinct sustained release behaviors, which are likely correlated to varying molecular interactions of matrine, oxymatrine, and sophoridine with resveratrol, as well as the unexpected recrystallization of resveratrol from the co-amorphous systems on the surface of drug tablets. Our study not only results in three new co-amorphous drug systems with great anti-COVID-19 potential, but also suggests a promising translational route for natural products from traditional Chinese medicines.

## 2. Materials and Methods

### 2.1. Materials

All compounds used in this study were from commercial sources and used as received, including matrine ( $\geq 98\%$ ), oxymatrine ( $\geq 96\%$ ), and sophoridine ( $\geq 99\%$ ) (Bide Pharmatech, Shanghai, China) and resveratrol ( $\geq 99\%$ ) (Aladdin, Shanghai, China). All other chemical reagents were from Sinopharm Chemical Reagent (Shanghai, China).

### 2.2. Preparation of the Co-Amorphous Systems

The solvent evaporation method was applied for preparation of the co-amorphous systems. Briefly, the mixture of crystalline matrine and crystalline resveratrol with molar ratio of 1:1 (0.2 mmol) was dissolved in 5 mL of methanol, followed by rotary vacuum evaporation at 50 °C. The resulting samples were collected and dried under vacuum at 30 °C for 24 h to remove the residual solvent and stored under a dry environment at room temperature for further investigation. The co-amorphous systems of oxymatrine and sophoridine with resveratrol were similarly prepared.

### 2.3. Solid-State Characterization

#### 2.3.1. PXRD

The PXRD spectra of all samples were recorded on a Bruker D8 Advance X-ray powder diffractometer with a Cu K $\alpha$  radiation ( $\lambda = 1.5406 \text{ \AA}$ ) source at 25 °C. The process parameters were set at a tube voltage of 40 kV and amperage of 40 mA. The tested samples were placed in monocrystalline sample disks. For each sample, the data were collected in a  $2\theta$  range of 3–40° with a step length of 0.0194° at a scanning speed of 0.1 s/step.

Mercury 3.8 was used to calculate the simulated PXRD pattern of oxymatrine trihydrate based on its single crystal data (No. 2058431) downloaded from the Cambridge Crystallographic Data Centre.

#### 2.3.2. mDSC

The thermodynamic behaviors of all crystalline samples and three co-amorphous samples were characterized using a TA Discovery 250 differential scanning calorimeter (TA Instruments, New Castle, DE, USA). Calibration of the instrument was carried out using indium as a standard, and sapphire disks were used for  $T_{\text{zero}}$  calibration. Each sample (3–5 mg) was placed in an aluminum pan, followed by heating at a scan rate of 2 K·min<sup>-1</sup> under a dry nitrogen purge ( $\geq 99.999\%$ ) at a flow rate of 50 mL·min<sup>-1</sup>. The samples were scanned from 30 to 200 °C (oxymatrine was scanned from 30 to 230 °C; resveratrol was scanned from 30 to 300 °C) with an amplitude of 1.00 °C and a period of 60 s.

#### 2.3.3. FTIR

An IR spectrophotometer (Nicolet Impact 410, Thermo Fisher, Waltham, MA, USA) was employed to record the FTIR spectra of all the samples. About 2 mg of each sample was mixed with 200 mg of potassium bromide (spectral grade purity) and compressed into tablets at room temperature. The FTIR spectra data were collected over the wavenumber range of 400–4000 cm<sup>-1</sup> with a distinguishing ability of 4 cm<sup>-1</sup>.

## 2.4. NMR

The  $^1\text{H}$ -NMR and  $^{13}\text{C}$ -NMR spectra of crystalline matrine, oxymatrine, sophoridine, resveratrol, and the three co-amorphous samples were recorded using an AVANCE III 400 MHz NMR spectrometer with  $\text{DMSO-}d_6$  as a solvent at  $25\text{ }^\circ\text{C}$ .

## 2.5. Dissolution Experiments

### 2.5.1. Equilibrium Solubility Determination

Equilibrium solubility experiments of crystalline forms of matrine, oxymatrine, sophoridine, and the three co-amorphous forms were performed. Excess quantity of each sample was weighed and added into a vial containing 1 mL phosphate buffer saline (PBS) (pH 6.8). The obtained suspension was stirred at 500 rpm in a water bath for 72 h with temperature of  $37 \pm 0.5\text{ }^\circ\text{C}$  and filtered by a  $0.22\text{ }\mu\text{m}$  polycarbonate filter. Then, the filtrate was diluted with fresh PBS to an appropriate concentration for high-performance liquid chromatography (HPLC) analysis. Each experiment was repeated three times.

### 2.5.2. In Vitro Release Experiment

The release behaviors of matrine, oxymatrine, and sophoridine, as well as the co-amorphous samples, were investigated by the paddle method. The powder samples contained 50 mg of matrine, oxymatrine, and sophoridine were accurately weighed and compressed at a pressure of 6 MPa to obtain tablets with 8 mm diameter for the release experiments. The release experiments were carried out in a dissolution tester (RC-6, Tianguang, Tianjin, China) at a rotational speed of 50 rpm in PBS (100 mL, pH = 6.8) as a dissolution medium at  $37 \pm 0.5\text{ }^\circ\text{C}$ . At the predetermined time points (1, 5, 10, 20, 30, 60, 120, 240, 360, and 720 min), the dissolution medium (1 mL) was acquired and the equal volume of fresh PBS was supplemented. The acquired sample was next filtrated through a polycarbonate filter ( $0.22\text{ }\mu\text{m}$ ), diluted with fresh PBS, and analyzed by HPLC. Triplicate experiments were conducted in parallel. At the end of release experiments, the tablets after release tests were collected and dried at room temperature. The solid samples on the surface and the core of the tablets were separately used for PXRD characterization.

Waters e2695 HPLC (ACQUITY Arc, Milford, MA, USA) equipped with a 2998 photodiode array detector and an AQ-C18 column ( $250\text{ mm} \times 4.6\text{ mm}$ ,  $5\text{ }\mu\text{m}$ ) was used. Matrine, oxymatrine and sophoridine were detected at UV absorption wavelengths of 220 nm. The mobile phase consisted of water (with 0.1% formic acid) and acetonitrile (50:50 *v/v*) at flow rate of  $1\text{ mL}\cdot\text{min}^{-1}$ .

## 2.6. Scanning Electron Microscopy

The surface morphology of the tablets before and after release tests were characterized by scanning electron microscopy (SEM) (FEI Czech Republic s.r.o. Quanta FEG 250, Columbia, MD, USA). The samples were mounted on aluminum stubs with double-sided sticky discs of conductive carbon, and then coated with gold, followed by microscopical scanning.

## 2.7. Physical Stability

All co-amorphous powders were exposed in desiccators contained anhydrous silica gel (low humidity condition) at  $25\text{ }^\circ\text{C}$  and  $40\text{ }^\circ\text{C}$  for physical stability evaluation. In addition, their physical stabilities were also studied at  $25\text{ }^\circ\text{C}$  under a saturated sodium chloride solution atmosphere (75% relative humidity (RH)) [33]. The powder samples were collected at a preset time and measured by PXRD. The physical stability of the three co-amorphous systems against pressure was also investigated under a pressure of 6 MPa for 10 min, resulting in the formation of a tablet. Each tablet was then crushed and characterized by PXRD.

### 3. Results and Discussion

#### 3.1. The Design and Preparation of Co-Amorphous Drug Systems of Matrine, Oxymatrine, and Sophoridine with Resveratrol and Their PXRD Characterization

We selected resveratrol as the co-former for the amorphization of matrine, oxymatrine, and sophoridine (Figure 1). In addition, the three quinolizidine alkaloids share the same structure scaffold, since oxymatrine is the *N*-oxide of matrine, while sophoridine is the C-5 epimer of matrine. Although co-amorphous systems have become a promising approach in drug formulation [26,27], to our knowledge, many previously studied systems include a single small molecule drug with one or multiple co-formers. The study of the molecular interactions in these systems have largely focused on the varying interactions and physico-chemical properties of drugs and their co-formers, including amino acids, dipeptides, and phenolic acids, among others [34–36]. The high structure similarity of matrine, oxymatrine, and sophoridine provides a rare opportunity to study their molecular interactions with the single co-former resveratrol, thus potentially offering new insights of the co-amorphous drug systems.

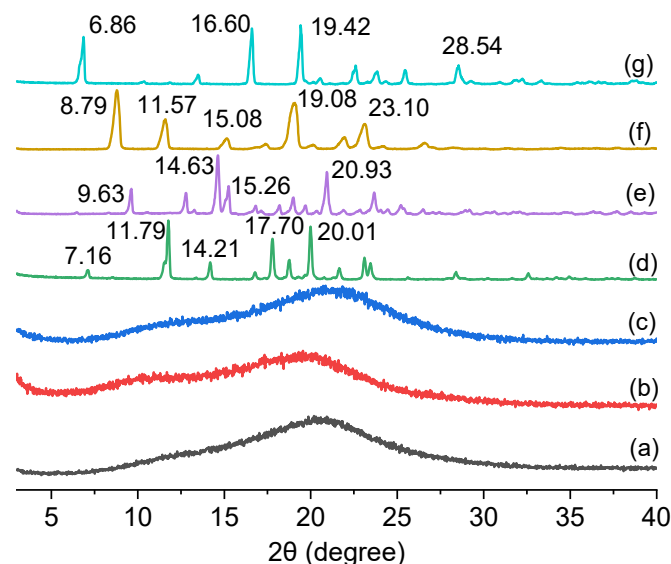


**Figure 1.** The PXRD patterns of co-amorphous forms of MAR-RES (a), OMAR-RES (b), and SPD-RES (c), as well as crystalline forms of matrine (d), oxymatrine (e), sophoridine (f), and resveratrol (g).

We adopted the solvent evaporation method to prepare the co-amorphous systems of matrine, oxymatrine, and sophoridine with resveratrol. We next evaluated the PXRD patterns of the prepared solids, including MAR-RES, OMAR-RES, and SPD-RES, through the powder X-ray diffraction analysis, using their respective crystalline forms as controls. For the crystalline forms of matrine, oxymatrine, sophoridine, and resveratrol (Figure 1d–g), characteristic diffraction peaks ((7.16°, 11.79°, 14.21°, 17.70°, and 20.01°), (9.63°, 14.63°, 15.26°, and 20.93°), (8.79°, 11.57°, 15.08°, 19.08°, and 23.10°) and (6.86°, 16.60°, 19.42°, and 28.54°), respectively) appeared at  $2\theta$  over 3–40°. The crystalline oxymatrine was confirmed as a trihydrate, since its PXRD pattern was in line with the simulated one using the single crystal data of oxymatrine trihydrate (Figure S1) [37]. In contrast, the three solid samples of matrine, oxymatrine, and sophoridine that co-evaporated with resveratrol exhibited a typical halo with no characteristic peaks (Figure 1a–c), suggesting that all of them were transformed into an amorphous state. However, we were unable to prepare the amorphous forms of matrine, oxymatrine, sophoridine, and resveratrol under the same condition (Figure S2). The PXRD pattern of evaporated oxymatrine exhibited certain differences with its original crystalline form, indicating a polymorphism (oxymatrine monohydrate) formed after treatment (Figure S2c–d) [37], while other parent materials evaporated alone showed no phase transition.

### 3.2. mDSC Study of the Amorphous MAR-RES, OMRA-RES, and SPD-RES Samples

In order to investigate the formation of co-amorphous systems, the mDSC curves of the amorphous MAR-RES, OMRA-RES, and SPD-RES samples were obtained by mDSC, along with their individual crystalline form as controls (Figure 2). The crystalline forms of matrine, sophoridine, and resveratrol exhibited endothermic melting peaks at 85.59 °C, 108.89 °C, and 265.05 °C, respectively. Crystalline oxymatrine manifested three endothermic peaks at 57.57 °C, 161.21 °C, and 205.12 °C, respectively [38]. The first endothermic peak corresponded to the phase transition from trihydrate to monohydrate of oxymatrine and the second endothermic peak suggested that the oxymatrine monohydrate transformed into anhydrous oxymatrine. The third endothermic peak was the melting peak of anhydrous oxymatrine [37]. Different from their crystalline counterparts, the co-evaporated samples of MRA-RES, OMAR-RES, and SPD-RES displayed single glass transition temperature ( $T_g$ ) at 72.44 °C, 134.13 °C, and 93.83 °C, respectively, which supports the formation of homogeneous co-amorphous systems. Obviously, co-amorphous OMAR-RES showed much higher  $T_g$ , compared to the other two co-amorphous systems, indicating that it may hold stronger intermolecular interactions.

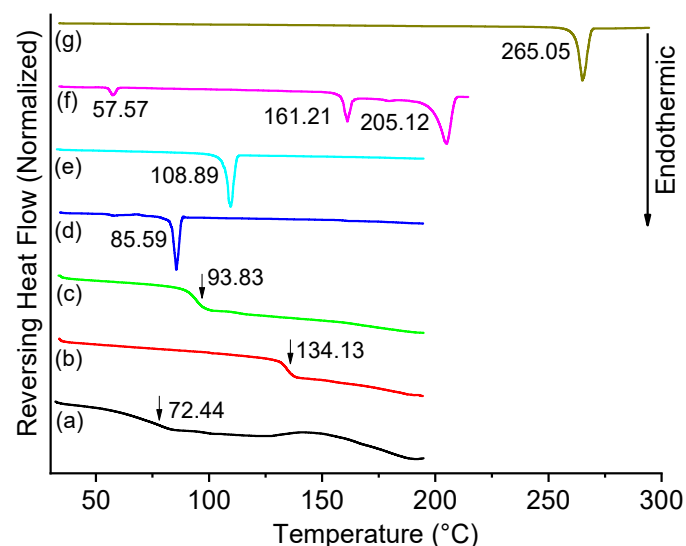


**Figure 2.** The mDSC curves of co-amorphous forms of MAR-RES (a), OMAR-RES (b), and SPD-RES (c), as well as crystalline forms of matrine (d), oxymatrine (e), sophoridine (f), and resveratrol (g).

### 3.3. FTIR

FTIR is an analytical technique used to study the interactions among drugs and co-formers in co-amorphous drug systems, due to its ability to detect characteristic vibrations of chemical bonds by inelastic collisions between tested samples and infrared light. Therefore, the FTIR spectra of co-amorphous MAR-RES, OMRA-RES, and SPD-RES, as well as their crystalline forms and physical mixtures were obtained (Figures 3 and S3–S10). The crystalline matrine showed a typical C=O stretching vibration ( $\nu(\text{C}=\text{O})$ ) of the lactam functional group at 1646  $\text{cm}^{-1}$  and a C–H stretching vibration from methylene groups in 2937  $\text{cm}^{-1}$  (Figure 3d). Its characteristic C–N stretching vibration ( $\nu(\text{C}-\text{N})$ ) peaks appeared at 1415  $\text{cm}^{-1}$ , consistent with the previous report [39]. The crystalline sophoridine exhibited the similar FTIR spectrum with matrine, with representative peaks of  $\nu(\text{C}=\text{O})$  and  $\nu(\text{C}-\text{N})$  in 1620  $\text{cm}^{-1}$  and 1416  $\text{cm}^{-1}$ , respectively (Figure 3f). In contrast, the crystalline oxymatrine had peaks in 2286  $\text{cm}^{-1}$  and 1609  $\text{cm}^{-1}$  [40], which are attributed to  $\text{N}^+-\text{O}^-$  stretching vibration ( $\nu(\text{N}^+-\text{O}^-)$ ) and  $\nu(\text{C}=\text{O})$  of the lactam, respectively (Figures 3e and S4). The crystalline resveratrol manifested broad stretching vibration signals of the phenolic hydroxyl groups ( $\nu(\text{O}-\text{H})$ ) at 3240  $\text{cm}^{-1}$ , and representative peaks at 1605  $\text{cm}^{-1}$ , 1586  $\text{cm}^{-1}$ , and 1443  $\text{cm}^{-1}$  belonging to C–C stretching vibrations and planar C–C–H deformation vibrations of the two benzene moieties (Figure 3g). A superposition of the spectra of the pure

components was observed in the three physical mixtures, indicating that no intermolecular interactions occurred between the individual components (Figure S10).

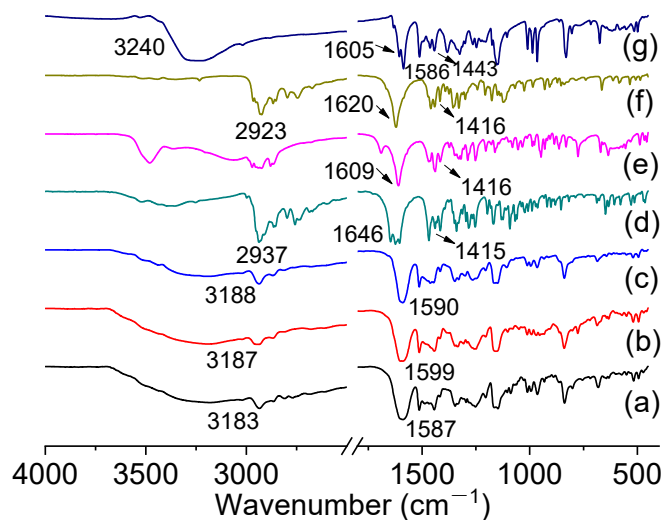


**Figure 3.** The FTIR spectra of co-amorphous forms of MAR-RES (a), OMAR-RES (b), and SPD-RES (c), as well as crystalline forms of matrine (d), oxymatrine (e), sophoridine (f), and resveratrol (g).

However, in the FTIR spectra of all co-amorphous samples, their characteristic peaks became broad and blunt compared to those of their crystalline counterparts (Figure 3a–c). For example, the sharp peak of  $\nu(\text{O-H})$  of resveratrol at  $3240\text{ cm}^{-1}$  was shifted to  $3183\text{ cm}^{-1}$ , while the  $\nu(\text{C=O})$  peak of matrine was shifted from  $1646\text{ cm}^{-1}$  to  $1587\text{ cm}^{-1}$ . The obvious broadened and shifted stretching vibration peaks of both matrine and resveratrol indicate that the intermolecular interactions may exist between matrine and resveratrol. Similar FTIR changes could also be observed in co-amorphous OMAR-RES and SPD-RES (Figure 3b,c). The significant broadening and shift of the peaks of  $\nu(\text{O-H})$  from  $3240\text{ cm}^{-1}$  to  $3187\text{ cm}^{-1}$  and  $\nu(\text{C=O})$  from  $1609\text{ cm}^{-1}$  shifted to  $1599\text{ cm}^{-1}$  in resveratrol and oxymatrine could be identified in the co-amorphous OMAR-RES, as well as the decreased  $\nu(\text{N}^+-\text{O}^-)$  signal in  $2286\text{ cm}^{-1}$  of oxymatrine (Figures 3b, S4 and S8). Similarly, the signals belonging to  $\nu(\text{O-H})$  of resveratrol and  $\nu(\text{C=O})$  of sophoridine at  $3240\text{ cm}^{-1}$  and  $1620\text{ cm}^{-1}$  were both shifted to  $3188\text{ cm}^{-1}$  and  $1590\text{ cm}^{-1}$ , respectively (Figure 3c). Taken together, these data suggest that there are certain intermolecular interactions between the O–H groups of resveratrol and the C=O group of the three tested alkaloids, while additional interactions may exist between the phenolic groups of resveratrol and the N-oxide of oxymatrine.

#### 3.4. The Molecular Interactions of Resveratrol and Oxymatrine in DMSO- $d_6$

The presence of molecular interactions in the above co-amorphous samples raised an interesting question of whether these interactions are also present in solution, which may affect their release behaviors and pharmacokinetics. Therefore, we opted to study co-amorphous MAR-RES, OMAR-RES, and SPD-RES in the aprotic solvent DMSO- $d_6$ , using  $^1\text{H}$  and  $^{13}\text{C}$  NMR spectroscopy (Figures 4 and S11–S13 and Tables S2–S4). The reason is that many of these interactions involve hydrogen bond interactions including the phenolic groups of resveratrol and the carbonyl group of the lactam ring in these alkaloids, along with the N-oxide functional group of oxymatrine. The peak assignment of matrine, oxymatrine, sophoridine, and resveratrol in their  $^1\text{H}$  NMR and  $^{13}\text{C}$  NMR spectra was summarized in the supporting information Tables S2–S4 [41–43]. There were slight changes of certain chemical shifts in MAR-RES and SPD-RES samples in their NMR spectra in comparison to their individual counterparts, suggesting negligible interactions between MAR-RES and SPD-RES under the tested conditions (Figures S11 and S12, Table S2). In contrast, significant changes of certain chemical shifts in co-amorphous OMAR-RES were observed in both the  $^1\text{H}$  NMR and  $^{13}\text{C}$  NMR spectra, compared to their crystalline counterparts in

DMSO- $d_6$  (Figures 4 and S13). For example, two series of phenolic groups of resveratrol were downfield shifted by 0.74 and 1.09 ppm to merge into a broad peak at  $\delta = 10.3$  ppm, suggesting a strong shielding effect probably by the formation of inter-molecular hydrogen bonds with oxymatrine, consistent with the downfield shifted signals of C-3, C-5, and C-4' of resveratrol in the  $^{13}\text{C}$  NMR spectrum of OMAR-RES (Table S4). In addition, the downfield shifted signals of H-2 and H-6 ( $\Delta\delta = \sim 0.2$  ppm) and C-6 ( $\Delta\delta = \sim 0.7$  ppm), and the upfield shifted signals of C-2, C-8, and C-10 ( $\Delta\delta = \sim 0.6, 0.4,$  and  $0.5$  ppm) from oxymatrine strongly suggesting that the hydrogen bond acceptor is the *N*-oxide in oxymatrine. Taken together, the unique *N*-oxide in oxymatrine in OMAR-RES seemed to impose the important intermolecular interaction with resveratrol in DMSO- $d_6$ .

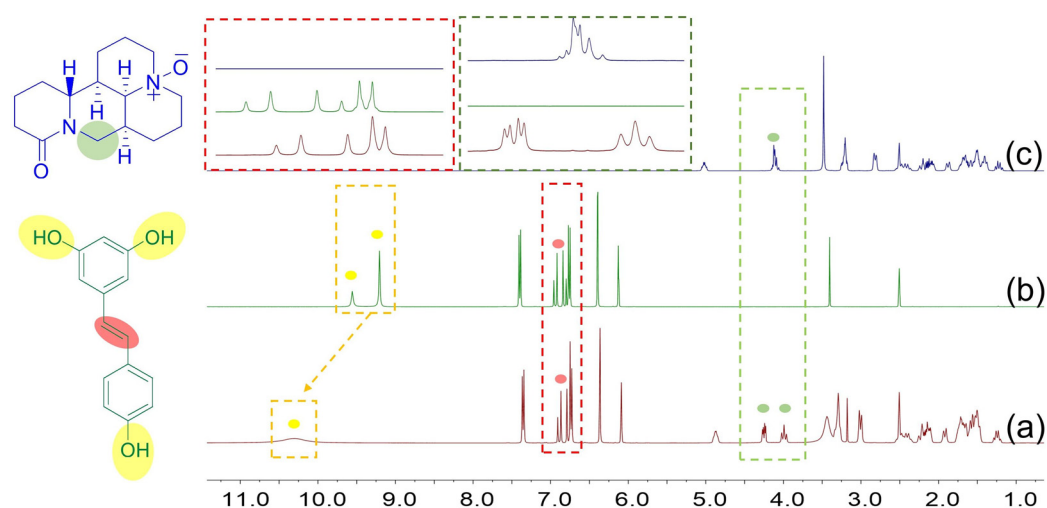


**Figure 4.** One-dimensional  $^1\text{H}$  NMR spectra of co-amorphous forms of OMAR-RES (a), resveratrol (b), and oxymatrine (c) dissolved in DMSO- $d_6$ .

### 3.5. Dissolution Experiments

We next determined the equilibrium solubility of matrine, oxymatrine, sophoridine in their co-amorphous systems with resveratrol (Figure 5a). The equilibrium solubility of the crystalline forms of matrine, oxymatrine, sophoridine was 55, 1642, and 1203 mg/mL at 37 °C in PBS buffer (pH 6.8), while their individual one in the co-amorphous systems was drastically reduced to 6.3, 7.6, and 6.9 mg/mL, respectively. In contrast, no resveratrol could be observed under the current tested conditions, probably due to its poor water solubility. We further evaluated the residue solids after these equilibrium solubility tests using PXRD (Figures S14–S16). Interestingly, only the diffraction peaks of resveratrol emerged and no diffraction signals of matrine-type alkaloids could be observed on the PXRD patterns of the samples after dissolution tests. The diffraction peaks in Figure S16c are weaker than those of other two co-amorphous samples (Figures S14c and S15c) after dissolution and marked with asterisks for clarity. The recrystallization of resveratrol in the co-amorphous systems may be more significantly interfered with by sophoridine in comparison to the other two co-amorphous systems. The observed typical halo in PXRD suggests the presence of the remaining co-amorphous solids in the tested samples.



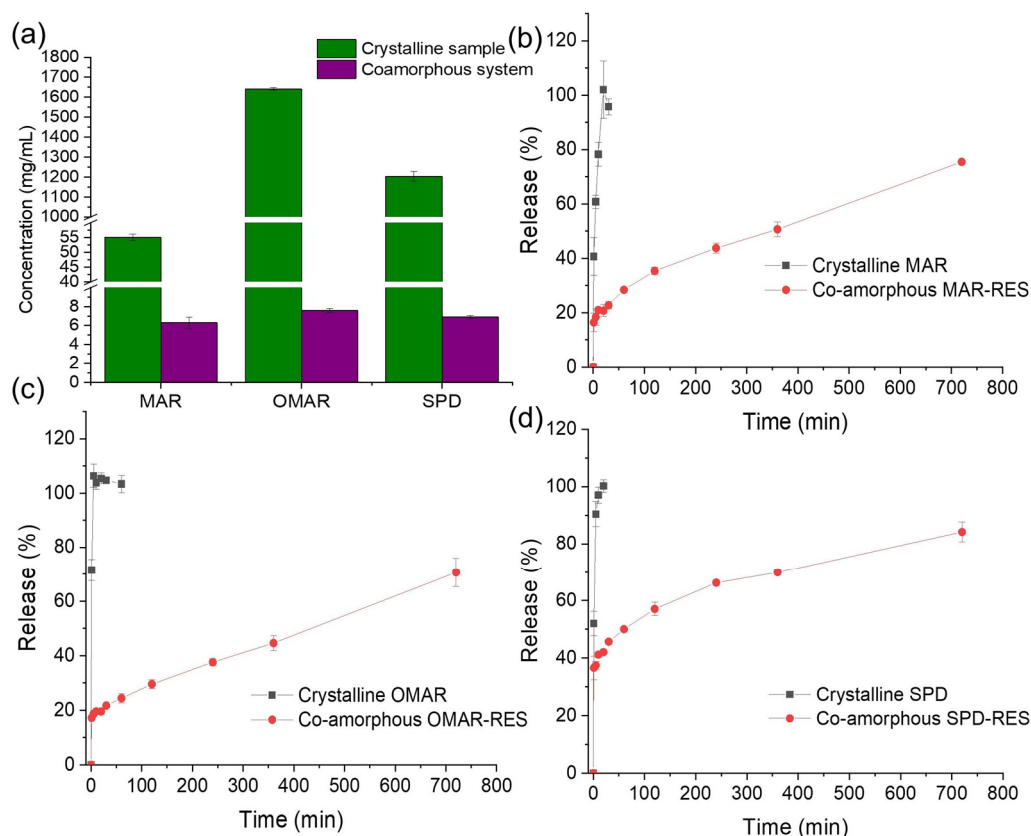


**Figure 5.** Equilibrium solubilities of matrine, oxymatrine, and sophoridine from their crystalline and co-amorphous forms (a); release profiles of MAR from crystalline MAR and co-amorphous MAR-RES (b); OMAR from crystalline OMAR and co-amorphous OMAR-RES (c); SPD from crystalline SPD, and co-amorphous SPD-RES (d) in pH 6.8 PBS at  $37 \pm 0.5$  °C.

The *in vitro* release behaviors of the three co-amorphous systems and their crystalline counterparts were next studied (Figure 5b–d). Matrine, oxymatrine, and sophoridine displayed sustained release behavior from their co-amorphous forms, compared to the crystalline one. For example, the crystalline matrine released totally within 30 min, while only up to ~75% of matrine released from the co-amorphous MAR-RES after 12 h (Figure 5b). The crystalline oxymatrine and sophoridine also released rapidly and reached almost 100% cumulative release within 30 min (Figure 5c,d). However, ~71% of oxymatrine and ~84% of sophoridine released from their co-amorphous systems after 12 h. It appeared that oxymatrine released the slowest among the three co-amorphous systems, probably due to the stronger interactions between oxymatrine and resveratrol. Interestingly, sophoridine released the fastest from co-amorphous SPD-RES among the tested co-amorphous systems during the first 5 min, with ~35% released sophoridine into the solution, in comparison to ~20% released matrine or oxymatrine from their respective co-amorphous systems, which may be because sophoridine does not have such strong molecular interactions in the liquid state as oxymatrine and resveratrol. This result suggests that resveratrol might be an excellent co-former in co-amorphous drug systems for the sustained release of potential drugs.

After the release experiments, the morphology of the residue tablets was examined, revealing that the surface and the inside of tablets were in two different states, since the tablet surface was brown-colored, dense, and easy to peel off. SEM study revealed that all of the residual tablets inside had round edges and smooth surfaces-like fragments, which were similar to the co-amorphous powder prepared by the same method (Figure S17a–c) [44]. In contrast, the SEM images of the tablet surface showed a rough, irregular, and angular morphology, suggesting the occurrence of recrystallization (Figure S17d–f), which was next

confirmed to be crystalline resveratrol by PXRD analysis, while all of the interior tablets kept the amorphous solid state (Figures S18–S20).

Therefore, we reasoned that there might be a distinct release mechanism of the three matrine-type alkaloids in their co-amorphous systems (Figure 6). The slow-release behavior due to gel formation has been studied in (co)-amorphous lurasidone hydrochloride, indomethacin/paracetamol, sinomenine with phenolic acids, and nonsteroidal anti-inflammatory drugs [28,32,33]. Qian and co-workers proposed that the gel formation was mediated by charge-assisted hydrogen bond formation [30]. In contrast, we discovered that the highly soluble alkaloids, e.g., matrine, rapidly dissolved from the tablet surface, resulting in the accumulation of an abundant amount of recrystallized resveratrol on the outer layer of tablets in contact with the aqueous solution (Figure S17). However, the interior portions of the tablets remained in an amorphous state (Figures S18d–S20d). The observed sustained release of matrine, oxymatrine, and sophoridine is likely because the recrystallization of resveratrol significantly limited the access of the PBS buffer to the co-amorphous systems inside the tablets (Figures S17–S20). The crystallized resveratrol on the surface of co-amorphous samples during the dissolution process may have formed a “shell-like” structure for the sustained release of matrine-type alkaloids.

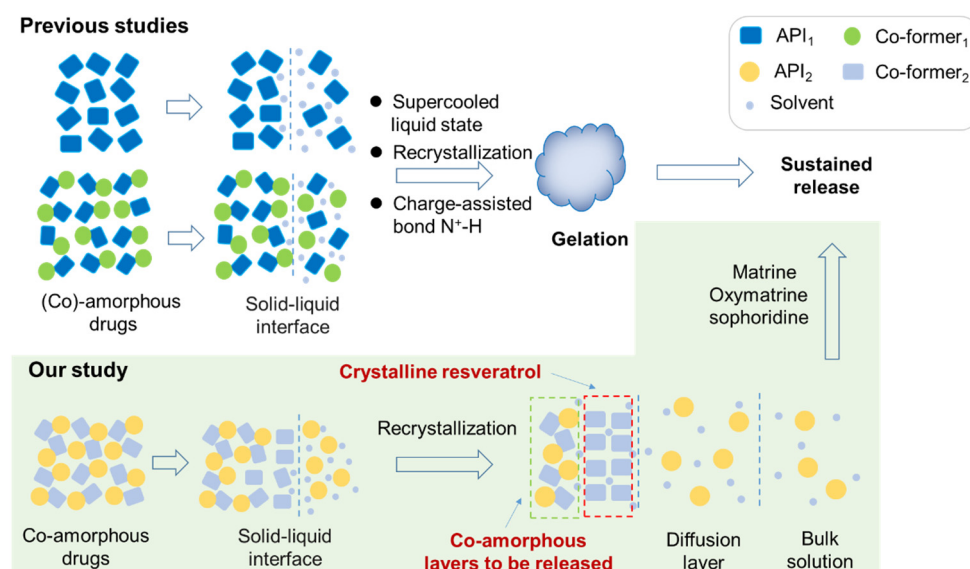


**Figure 6.** The proposed sustained-release mechanism for co-amorphous matrine/oxymatrine/sophoridine and resveratrol, in comparison to previously reported gelation-based release mechanism.

### 3.6. Physical Stability

The physical stability of the three co-amorphous drug systems were evaluated under three conditions (i.e., 25 °C, 40 °C/low RH, or 25 °C/75% RH) (Figures S21 and S22). Under 25 °C/low RH condition, all the tested co-amorphous samples maintained their amorphous solid-state after nine months of storage (Figure S21). Under accelerated storage condition (40 °C/low RH or 25 °C/75% RH), no diffraction peaks were found in these samples after 4 or 2 months, respectively (Figure S22). This result suggests that the tested co-amorphous samples possess excellent physicochemical stability under all experimental conditions.

In order to study if recrystallization of the three co-amorphous samples occurred after compression, the compressed samples were next investigated by PXRD. As shown in Figure S23, no diffraction peaks appeared in the PXRD patterns of all the tested co-amorphous samples after compressed under the pressure of 937.5 MPa, suggesting their promising mechanical stability.

#### 4. Conclusions

Repurposing known drugs is an efficient approach to the fight against SARS-CoV-2. Based on the encouraging observational study of matrine for COVID-19, we prepared and evaluated the MAR-RES co-amorphous drug system, together with OMAR-RES and SPD-RES. We discovered that the three co-amorphous systems showed sustained release behavior, enabling the future development and clinical evaluation of a more convenient oral delivery route than continuous infusion for these excellent drug candidates against SARS-CoV-2. The crystallized resveratrol on the surface of co-amorphous samples during the dissolution process formed a “shell-like” structure, which may hinder the release of matrine-type alkaloids and realizes the sustained release. In addition, the similar yet structurally distinct interactions of matrine, oxymatrine, and sophoridine with the co-former resveratrol suggest that intermolecular interactions play a prominent role in their release. Considering the salient biological activity of resveratrol, it may be used as a new type of drug co-former in the preparation of co-amorphous drug samples. However, the recrystallization of resveratrol prevents its release under the tested conditions, resulting in no solubility improvement. Therefore, further studies are also needed to improve the release behavior of resveratrol, as well as the pharmacokinetics and therapeutic effects of the above co-amorphous systems in animal models.

**Supplementary Materials:** The following supporting information can be downloaded at: <https://www.mdpi.com/article/10.3390/pharmaceutics14030603/s1>. Table S1: The commercial drug formulations of matrine, oxymatrine, and sophoridine on the markets in China. Tables S2 and S3: The  $^1\text{H}$  NMR chemical shifts changes of MAR, SPD, OMAR and RES in  $\text{DMSO-}d_6$  after co-amorphization. Table S4: The  $^{13}\text{C}$  NMR chemical shifts changes of OMAR and RES in  $\text{DMSO-}d_6$  after co-amorphization. Figure S1: PXRD patterns of raw material OMAR (a), simulated of OMAR monohydrate (b) and OMAR trihydrate (c) derived from the single crystal structure. Figure S2: PXRD patterns of crystalline samples and the sample after rotary evaporation. Figures S3–S10: FTIR spectra of crystalline MAR, OMAR, SPD, the three co-amorphous forms, and their physical mixtures. Figures S11 and S12: The comparison of  $^1\text{H}$  NMR spectra of the co-amorphous forms of MAR-RES and SPD-RES dissolved in  $\text{DMSO-}d_6$ . Figure S13: The comparison of  $^{13}\text{C}$  NMR spectra of co-amorphous forms of OMAR-RES dissolved in  $\text{DMSO-}d_6$ . Figures S14–S16: PXRD patterns of three co-amorphous forms after the equilibrium solubility test. Figure S17: SEM images of the powder samples. Figures S18–S20: PXRD patterns of three co-amorphous forms after release tests. Figure S21: PXRD patterns of three CASs. Figure S22: The physicochemical stability of the three co-amorphous systems. Figure S23: PXRD patterns of three co-amorphous systems after pressure tests.

**Author Contributions:** D.H.: conceptualization, methodology, formal analysis, writing—original draft, writing—review and editing. X.C.: conceptualization, methodology, formal analysis, writing—review and editing. D.L.: methodology, formal analysis. H.Z.: formal analysis, writing—review and editing. Y.D.: conceptualization, funding acquisition. Y.H.: conceptualization, formal analysis, funding acquisition, writing—original draft, writing—review and editing. All authors have read and agreed to the published version of the manuscript.

**Funding:** This work was supported in part by the National Natural Science Foundation of China (82173688), the Chinese Ministry of Education 111 Project (BP0820034), the Guangdong Basic and Applied Basic Research Foundation (2019A1515110336), The Science and Technology Innovation Program of Hunan Province (2021RC4067), and Hunan Provincial Natural Science Foundation of China (2021JJ30791).

**Institutional Review Board Statement:** Not applicable.

**Informed Consent Statement:** Not applicable.

**Data Availability Statement:** Not applicable.

**Acknowledgments:** We are grateful to the Center for Advanced Research in CSU for the NMR experiments.

**Conflicts of Interest:** The authors declare no conflict of interest.

## References

1. WHO Coronavirus (COVID-19). Dashboard. Available online: <https://covid19.who.int/> (accessed on 10 December 2021).
2. COVID-19 Vaccines. Available online: <https://www.who.int/emergencies/diseases/novel-coronavirus-2019/covid-19-vaccines> (accessed on 10 December 2021).
3. Riva, L.; Yuan, S.F.; Yin, X.; Martin-Sancho, L.; Matsunaga, N.; Pache, L.; Burgstaller-Muehlbacher, S.; De Jesus, P.D.; Teriete, P.; Hull, M.V.; et al. Discovery of SARS-CoV-2 antiviral drugs through large-scale compound repurposing. *Nature* **2020**, *586*, 113–119. [[CrossRef](#)] [[PubMed](#)]
4. Jang, W.D.; Jeon, S.; Kim, S.; Lee, S.Y. Drugs repurposed for COVID-19 by virtual screening of 6218 drugs and cell-based assay. *Proc. Natl. Acad. Sci. USA* **2021**, *118*, e2024302118. [[CrossRef](#)] [[PubMed](#)]
5. Christy, M.P.; Uekusa, Y.; Gerwick, L.; Gerwick, W.H. Natural products with potential to treat RNA virus pathogens including SARS-CoV-2. *J. Nat. Prod.* **2021**, *84*, 161–182. [[CrossRef](#)] [[PubMed](#)]
6. Fu, L.F.; Shao, S.; Feng, Y.; Ye, F.; Sun, X.; Wang, Q.L.; Yu, F.; Wang, Q.S.; Huang, B.Y.; Niu, P.H.; et al. Mechanism of microbial metabolite leupeptin in the treatment of COVID-19 by traditional chinese medicine herbs. *mBio* **2021**, *12*, e0222021. [[CrossRef](#)] [[PubMed](#)]
7. Weng, J.-K. Plant solutions for the COVID-19 pandemic and beyond: Historical reflections and future perspectives. *Mol. Plant.* **2020**, *13*, 803–807. [[CrossRef](#)]
8. Li, X.; Tang, Z.W.; Wen, L.; Jiang, C.; Feng, Q.S. Matrine: A review of its pharmacology, pharmacokinetics, toxicity, clinical application and preparation researches. *J. Ethnopharmacol.* **2021**, *269*, 113682. [[CrossRef](#)]
9. Yang, M.W.; Chen, F.; Zhu, D.J.; Li, J.Z.; Zhu, J.L.; Zeng, W.; Qu, S.L.; Zhang, Y. Clinical efficacy of Matrine and Sodium Chloride Injection in treatment of 40 cases of COVID-19 (in Chinese). *Zhongguo Zhong Yao Za Zhi* **2020**, *45*, 2221–2231. [[CrossRef](#)]
10. Zuniga, M.; Gomes, C.; Carsons, S.E.; Bender, M.T.; Cotzia, P.; Miao, Q.R.; Lee, D.C.; Rodriguez, A. Autoimmunity to annexin A2 predicts mortality among hospitalised COVID-19 patients. *Eur. Resp. J.* **2021**, *58*, 2100918. [[CrossRef](#)]
11. Patil, P.; Shetty, P.; Kuriakose, N.; Gollapalli, P.; Shetty, S.; Bhandary, R.; Vishwanatha, J.K.; Ghate, S.D. Molecular insights on the possible role of Annexin A2 in COVID-19 pathogenesis and post-infection complications. *Int. J. Mol. Sci.* **2021**, *22*, 1028. [[CrossRef](#)]
12. Wang, D.Y.; Cao, Y.; Zheng, L.Y.; Lv, D.Y.; Chen, L.D.; Xing, X.R.; Zhu, Z.Y.; Li, X.Y.; Chai, Y.F. Identification of Annexin A2 as a target protein for plant alkaloid matrine. *Chem. Commun.* **2017**, *53*, 5020–5023. [[CrossRef](#)]
13. Ye, X.W.; Deng, Y.L.; Zhang, X.; Liu, M.M.; Liu, Y.; Xie, Y.T.; Wan, Q.; Huang, M.; Zhang, T.; Xi, J.H.; et al. Study on the mechanism of treating COVID-19 with Shenqi Wan based on network pharmacology. *Drug Dev. Ind. Pharm.* **2021**. Online ahead of print. [[CrossRef](#)] [[PubMed](#)]
14. Liu, F.Z.; Li, Y.B.; Yang, Y.; Li, M.; Du, Y.; Zhang, Y.Y.; Wang, J.; Shi, Y.J. Study on mechanism of matrine in treatment of COVID-19 combined with liver injury by network pharmacology and molecular docking technology. *Drug Deliv.* **2021**, *28*, 325–342. [[CrossRef](#)] [[PubMed](#)]
15. Peng, W.P.; Xu, Y.; Han, D.; Feng, F.C.; Wang, Z.C.; Gu, C.; Zhou, X.M.; Wu, Q. Potential mechanism underlying the effect of matrine on COVID-19 patients revealed through network pharmacological approaches and molecular docking analysis. *Arch. Physiol. Biochem.* **2020**. Online ahead of print. [[CrossRef](#)] [[PubMed](#)]
16. Li, Y.; Wang, G.; Liu, J.; Ouyang, L. Quinolizidine alkaloids derivatives from *Sophora alopecuroides* Linn: Bioactivities, structure-activity relationships and preliminary molecular mechanisms. *Eur. J. Med. Chem.* **2020**, *188*, 111972. [[CrossRef](#)] [[PubMed](#)]
17. Wang, R.Z.; Deng, X.X.; Gao, Q.X.; Wu, X.L.; Han, L.; Gao, X.L.; Zhao, S.P.; Chen, W.B.; Zhou, R.R.; Li, Z.Y.; et al. *Sophora alopecuroides* L.: An ethnopharmacological, phytochemical, and pharmacological review. *J. Ethnopharmacol.* **2020**, *248*, 112172. [[CrossRef](#)]
18. Dai, J.P.; Wang, Q.W.; Su, Y.; Gu, L.M.; Deng, H.X.; Chen, X.X.; Li, W.Z.; Li, K.S. Oxymatrine inhibits influenza A virus replication and inflammation via TLR4, p38 MAPK and NF-kappa B pathways. *Int. J. Mol. Sci.* **2018**, *19*, 965. [[CrossRef](#)]
19. Ren, G.; Ding, G.T.; Zhang, H.Y.; Wang, H.P.; Jin, Z.J.; Yang, G.X.; Han, Y.H.; Zhang, X.; Li, G.Y.; Li, W.H. Antiviral activity of sophoridine against enterovirus 71 in vitro. *J. Ethnopharmacol.* **2019**, *236*, 124–128. [[CrossRef](#)]
20. McCreary, M.R.; Schnell, P.M.; Rhoda, D.A. Randomized double-blind placebo-controlled proof-of-concept trial of Resveratrol for outpatient treatment of mild coronavirus disease (COVID-19). *Res. Sq.* **2021**. Preprint. [[CrossRef](#)]
21. Liao, M.T.; Wu, C.C.; Wu, S.F.V.; Lee, M.C.; Hu, W.C.; Tsai, K.W.; Yang, C.H.; Lu, C.L.; Chiu, S.K.; Lu, K.C. Resveratrol as an adjunctive therapy for excessive oxidative stress in aging COVID-19 patients. *Antioxidants* **2021**, *10*, 1440. [[CrossRef](#)]
22. Yang, Z.; Gao, S.; Yin, T.J.; Kulkarni, K.H.; Teng, Y.; You, M.; Hu, M. Biopharmaceutical and pharmacokinetic characterization of matrine as determined by a sensitive and robust UPLC-MS/MS method. *J. Pharm. Biomed. Anal.* **2010**, *51*, 1120–1127. [[CrossRef](#)]
23. Tang, L.; Dong, L.N.; Peng, X.J.; Li, Y.; Shi, J.; Zhou, F.Y.; Liu, Z.Q. Pharmacokinetic characterization of oxymatrine and matrine in rats after oral administration of radix *Sophorae tonkinensis* extract and oxymatrine by sensitive and robust UPLC-MS/MS method. *J. Pharm. Biomed. Anal.* **2013**, *83*, 179–185. [[CrossRef](#)] [[PubMed](#)]
24. Chen, M.C.; Jiang, Q.; Zhang, M.Y.; Chen, S.Y.; Lou, J.S.; Chen, Y.J.; Wang, F.; Wang, R.Y. Establishment of quantitative methodology for sophoridine analysis and determination of its pharmacokinetics and bioavailability in rat. *Drug Dev. Ind. Pharm.* **2021**, *47*, 741–747. [[CrossRef](#)] [[PubMed](#)]
25. Shi, Q.; Moinuddin, S.M.; Cai, T. Advances in coamorphous drug delivery systems. *Acta Pharm. Sin. B* **2019**, *9*, 19–35. [[CrossRef](#)] [[PubMed](#)]

26. Han, J.W.; Wei, Y.F.; Lu, Y.; Wang, R.Z.; Zhang, J.J.; Gao, Y.; Qian, S. Co-amorphous systems for the delivery of poorly water-soluble drugs: Recent advances and an update. *Expert Opin. Drug Deliv.* **2020**, *17*, 1411–1435. [[CrossRef](#)]
27. Fael, H.; Demirel, A.L. Indomethacin co-amorphous drug-drug systems with improved solubility, supersaturation, dissolution rate and physical stability. *Int. J. Pharm.* **2021**, *600*, 120448. [[CrossRef](#)]
28. Li, B.; Hu, Y.; Wu, T.; Feng, Y.; Jiang, C.P.; Du, H.Z.; Lu, S. Apigenin-oxymatrine binary co-amorphous mixture: Enhanced solubility, bioavailability, and anti-inflammatory effect. *Food Chem.* **2021**, *373*, 131485. [[CrossRef](#)]
29. Heng, W.L.; Wei, Y.F.; Xue, Y.F.; Cheng, H.; Zhang, L.H.; Zhang, J.J.; Gao, Y.; Qian, S. Gel formation induced slow dissolution of amorphous Indomethacin. *Pharm. Res.* **2019**, *36*, 159. [[CrossRef](#)]
30. Qian, S.; Wang, S.S.; Li, Z.; Wang, X.J.; Ma, D.; Liang, S.J.; Gao, Y.; Zhang, J.J.; Wei, Y.F. Charge-assisted bond N(+)H mediates the gelation of amorphous lurasidone hydrochloride during dissolution. *Int. J. Pharm.* **2017**, *518*, 335–341. [[CrossRef](#)]
31. Chen, X.; Li, D.X.; Zhang, H.L.; Duan, Y.W.; Huang, Y. Co-amorphous systems of sinomenine with nonsteroidal anti-inflammatory drugs: A strategy for solubility improvement, sustained release, and drug combination therapy against rheumatoid arthritis. *Int. J. Pharm.* **2021**, *606*, 120894. [[CrossRef](#)]
32. Chen, X.; Li, D.X.; Zhang, H.L.; Duan, Y.W.; Huang, Y. Sinomenine-phenolic acid coamorphous drug systems: Solubilization, sustained release, and improved physical stability. *Int. J. Pharm.* **2021**, *598*, 120389. [[CrossRef](#)]
33. Bui, R.; Labat, M.; Aubert, J.E. Comparison of the saturated salt solution and the dynamic vapor sorption techniques based on the measured sorption isotherm of barley straw. *Constr. Build. Mater.* **2017**, *141*, 140–151. [[CrossRef](#)]
34. Lobmann, K.; Laitinen, R.; Strachan, C.; Rades, T.; Grohgan, H. Amino acids as co-amorphous stabilizers for poorly water-soluble drugs—Part 2: Molecular interactions. *Eur. J. Pharm. Biopharm.* **2013**, *85*, 882–888. [[CrossRef](#)]
35. Wu, W.Q.; Grohgan, H.; Rades, T.; Lobmann, K. Comparison of co-former performance in co-amorphous formulations: Single amino acids, amino acid physical mixtures, amino acid salts and dipeptides as co-formers. *Eur. J. Pharm. Sci.* **2021**, *156*. [[CrossRef](#)] [[PubMed](#)]
36. Fael, H.; Demirel, A.L. Tannic acid as a co-former in co-amorphous systems: Enhancing their physical stability, solubility and dissolution behavior. *Int. J. Pharm.* **2020**, *581*, 119284. [[CrossRef](#)] [[PubMed](#)]
37. Qi, M.H.; Li, H.; Zhu, B.; Hong, M.H.; Ren, G.B. Cocrystals of Oxymatrine: Reducing Hygroscopicity and Affecting the Dissolution Rate. *Cryst. Growth Des.* **2021**, *21*, 3874–3888. [[CrossRef](#)]
38. Yue, P.F.; Yuan, H.L.; Li, X.Y.; Yang, M.; Zhu, W.F. Process optimization, characterization and evaluation in vivo of oxymatrine-phospholipid complex. *Int. J. Pharm.* **2010**, *387*, 139–146. [[CrossRef](#)]
39. Ruan, J.H.; Liu, J.; Zhu, D.; Gong, T.; Yang, F.M.; Hao, X.J.; Zhang, Z.R. Preparation and evaluation of self-nanoemulsified drug delivery systems (SNEDDSs) of matrine based on drug-phospholipid complex technique. *Int. J. Pharm.* **2010**, *386*, 282–290. [[CrossRef](#)]
40. Li, B.; Hu, Y.; Guo, Y.J.; Xu, R.J.; Fang, X.P.; Xiao, X.C.; Jiang, C.P.; Lu, S. Coamorphous system of Florfenicol-Oxymatrine for improving the solubility and dissolution rate of Florfenicol: Preparation, characterization and molecular dynamics simulation. *J. Pharm. Sci.* **2021**, *110*, 2544–2554. [[CrossRef](#)]
41. Lei, W.; Xing-De, W.; Juan, H.; Gen-Tao, L.; Li-Yan, P.; Yan, L.; Liu-Dong, S.; Qin-Shi, Z. A new Quinolizidine alkaloid from *Sophora flavescens*. *Chem. Nat. Compd.* **2014**, *50*, 876–879. [[CrossRef](#)]
42. Hwang, J.S.; Lee, S.A.; Hong, S.S.; Lee, K.S.; Lee, M.K.; Hwang, B.Y.; Ro, J.S. Monoamine oxidase inhibitory components from the roots of *Sophora flavescens*. *Arch. Pharm. Res.* **2005**, *28*, 190–194. [[CrossRef](#)]
43. Pineda-Sanabria, S.E.; Robertson, I.M.; Sykes, B.D. Structure of trans-resveratrol in complex with the cardiac regulatory protein troponin C. *Biochemistry* **2011**, *50*, 1309–1320. [[CrossRef](#)] [[PubMed](#)]
44. Ali, A.M.A.; Ali, A.A.; Maghrabi, I.A. Clozapine-carboxylic acid plasticized co-amorphous dispersions: Preparation, characterization and solution stability evaluation. *Acta Pharm.* **2015**, *65*, 133–146. [[CrossRef](#)] [[PubMed](#)]